

Increasing importance of precipitation variability on global livestock grazing lands

Lindsey L. Sloat^{1*}, James S. Gerber¹, Leah H. Samberg¹, William K. Smith^{1,2}, Mario Herrero³, Laerte G. Ferreira⁴, Cécile M. Godde³ and Paul C. West¹

Pastures and rangelands underpin global meat and milk production and are a critical resource for millions of people dependent on livestock for food security^{1,2}. Forage growth, which is highly climate dependent^{3,4}, is potentially vulnerable to climate change, although precisely where and to what extent remains relatively unexplored. In this study, we assess climate-based threats to global pastures, with a specific focus on changes in within- and between-year precipitation variability (precipitation concentration index (PCI) and coefficient of variation of precipitation (CVP), respectively). Relating global satellite measures of vegetation greenness (such as the Normalized Difference Vegetation Index; NDVI) to key climatic factors reveals that CVP is a significant, yet often overlooked, constraint on vegetation productivity across global pastures. Using independent stocking data, we found that areas with high CVP support lower livestock densities than less-variable regions. Globally, pastures experience about a 25% greater year-to-year precipitation variation (CVP = 0.27) than the average global land surface area (0.21). Over the past century, CVP has generally increased across pasture areas, although both positive (49% of pasture area) and negative (31% of pasture area) trends exist. We identify regions in which livestock grazing is important for local food access and economies, and discuss the potential for pasture intensification in the context of long-term regional trends in precipitation variability.

Grazing lands produce forage over large areas that may be marginally or poorly suited for cropping or other activities, which allows ruminants to utilize primary productivity that is of limited direct value for human consumption. The utilization of natural pasture forages for livestock production relieves the pressure to convert, at a high environmental cost⁵, additional land to agriculture to produce supplemental feed. However, forage production on grazing lands is highly climate dependent and is therefore subject to alteration in the face of climatic change^{3,6}. The temporal and spatial heterogeneity of resources, particularly precipitation, has been linked to grazing land ecosystem dynamics through impacts on livestock carrying capacity and the potential for grassland degradation^{6,7}. Non-equilibrium concepts in rangeland ecology suggest that precipitation variability is a key driver of rangeland dynamics^{7–9}. An interannual CVP of 0.33 has been proposed as a threshold above which non-equilibrium conditions prevail⁷. Regions with a highly variable climate are subject to drought and deluge cycles that strongly affect vegetation production¹⁰. The impacts of changing climate on livestock grazing will probably be spatially variable, as projected changes include shifts

in long-term precipitation trends, the magnitude of precipitation events, changes in seasonality and changes in the timing of snow-melt, as well as increased year-to-year precipitation variability^{11,12}.

High levels of precipitation variability place limits on grazing livestock densities. The distribution of cattle on the landscape is related to CVP such that the more climatically stable areas (low CVP) also have the highest cattle densities (Fig. 1), independent of mean annual precipitation (MAP) (Supplementary Fig. 1). To examine this relationship spatially, we calculated and mapped CVP for global pasture areas (Supplementary Figures 1–3) concurrently with cattle densities (Methods gives the data set details and the Supplementary Information gives a map of CVP and agreement between the long-term station-derived precipitation Supplementary Data). Areas with intermediate (0.28–0.38) CVP (Fig. 1, yellow) may be of interest as they are more likely to be on or near ecosystem thresholds¹³. We find large swathes of these areas in the grazing lands of West and Southwest North America, parts of Argentina, Southern and Eastern Africa, Central Asia and Australia.

Precipitation variability acts as a key limiting factor on grazing capacity by constraining the annual vegetation productivity¹⁴. We found evidence in support of this idea by evaluating the relationships between CVP and NDVI. In general, areas with a high CVP have a low mean annual NDVI, whereas areas with low CVP experience a wide range of NDVI values, including the highest values of NDVI (Fig. 1, lower left, and Supplementary Fig. 5 gives additional details on the relationship between NDVI and CVP). We found this relationship even in areas of similar MAP (Supplementary Fig. 1). Additionally, CVP is a competitive explanatory climate variable for predicting NDVI. We ranked the frequency of retention of four commonly identified key climate variables—mean annual temperature (MAT), MAP, solar radiation and CVP—in the best Akaike information criterion (AIC)-selected model regressions of NDVI over time (1983–2010) for each 0.5° terrestrial grid cell. Globally, CVP was selected nearly as frequently as MAP and MAT (each best explaining ~21% of the global land area) and more frequently than solar radiation (~10% (Supplementary Table 1)). These results highlight the relative importance of CVP among other climate variables for constraining vegetation productivity. Supplementary Figs. 6 and 7 show global maps of the model results.

Overall, precipitation variability has increased across global pasture areas, although the maps reveal a patchwork of both positive and negative changes across the landscape (Fig. 2a). Trends in CVP between 1901 and 2014 were assessed using a sliding-window regression, with the coefficient of variation calculated in 25-year windows (details in are given in Methods and Supplementary Fig. 8).

¹Institute on the Environment, University of Minnesota, Saint Paul, MN, USA. ²School of Natural Resources and the Environment, University of Arizona, Tucson, AZ, USA. ³Commonwealth Scientific and Industrial Research Organization (CSIRO), St Lucia, Queensland, Australia. ⁴Image Processing and GIS Lab (Lapig), Federal University of Goiás, Campus Samambaia, Goiânia, Goiás, Brazil. *e-mail: lsloat@umn.edu

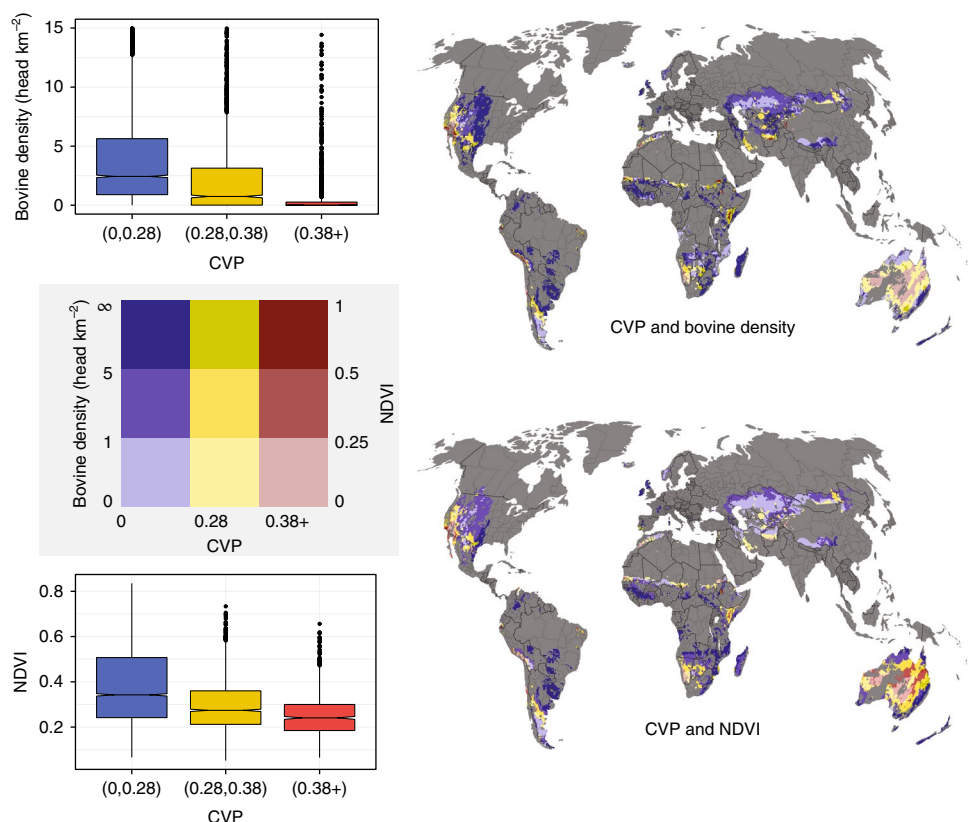


Fig. 1 | High year-to-year precipitation variability (CVP) is associated with lower cattle densities (upper left) and lower vegetation greenness (lower left).

CVP on global pastureland between 1982 and 2010 is mapped using colour whereas bovine density and NDVI for the same time period are mapped using colour intensity. CVP under 0.28 is mapped in blue, between 0.28 and 0.38 in yellow and above 0.38 in red. Bovine density and NDVI are divided into three bins that increase from the lightest to the darkest (bins 0, 1, 5 and infinity, and 0, 0.2, 0.5 and 1, respectively). There are significant differences between bovine density among each level of CVP and the same is true for NDVI and CVP (Tukey HSD (honest significant difference), $P < 0.001$). Boxplots display the distribution of bovine densities (top map) and NDVI (bottom map) within each CVP class (box, first and third quartile; black line, median; notches, family-wise 95% confidence interval).

This analysis revealed that of the total land area considered pasture in this study, 49% experienced increases in variability, 31% experienced decreases and 20% did not experience significant ($P < 0.05$) changes. Global pastures experience about a 25% larger CVP (0.27) than the average global land surface area excluding Antarctica (0.21). On the whole, CVP on global pastures increased by about 10% from 0.24 to 0.26 between 1901 and 2014. Trends in CVP summarized by region are given in Supplementary Fig. 9.

The variability of precipitation within years may also be important for livestock management, especially given that water availability is affected not only by the amount, but also by the concentration of precipitation events^{15,16}. To examine the magnitude of change in the intra-annual distribution of precipitation, we calculated the PCI¹⁷. The PCI indicates the amount of variation that occurs between the wettest and driest months. Notably, dependencies between CVP, PCI and MAP have been demonstrated at the global scale^{18,19} and we see these correlations in our analysis of global pasture areas (Supplementary Fig. 10). This is, in part, because within-year precipitation anomalies in places with a pronounced seasonality often influence the total annual precipitation, which then leads to a higher variability in interannual precipitation¹⁹. We used the same climate data and sliding-window approach to calculate changes in PCI from 1901 to 2014 (Fig. 2b). Areas with $PCI < 11$ are thought to have uniform, 11–16 moderate, 16–20 irregular, and over 20 strongly irregular precipitation distribution¹⁷. We found that, between 1901 and 2014, 45% of global pasturelands increased in PCI, 34% decreased and 21% did not significantly change ($P < 0.05$). Given that a

change in PCI of just a few points can mean the difference between a regular and irregular intra-annual precipitation distribution, the magnitude of changes in PCI over this period can be considered quite large in some areas (Fig. 3b). For example, the distribution of intra-annual precipitation has changed from uniform to irregular in parts of Northern Xinjiang Province and the Huánuco region of Central Peru. Changes in precipitation concentration, caused by a shift after the middle 1980s from a warm-and-dry state to a warm-and-wet state, were documented previously in Xinjiang, where the increasing precipitation intensity has contributed to the increasing frequency of damaging floods²⁰. PCI increases in Central Peru may be due to recent extreme precipitation events generally attributed to anomalies of the Intertropical Convergence Zone²¹. On the whole, intra-annual precipitation regimes appear to be increasing in irregularity in many of the same places that are also experiencing large interannual changes in precipitation. Maps that compare PCI at the beginning and the end of the time series are given in Supplementary Fig. 11.

To assess risks to places where livestock grazing is important for local food security, we used global data sets for percent pasture area (see Methods) and market influence²² (a combination of market access and per person purchasing power) to define areas in which livestock grazing may play a more or less important role in local food availability or the economy (Fig. 3). We found that areas where livestock grazing is an important part of local food availability (Fig. 3, dark red) and economies (dark blue) experience the highest levels of CVP (0.22 and 0.24, respectively), whereas areas where livestock

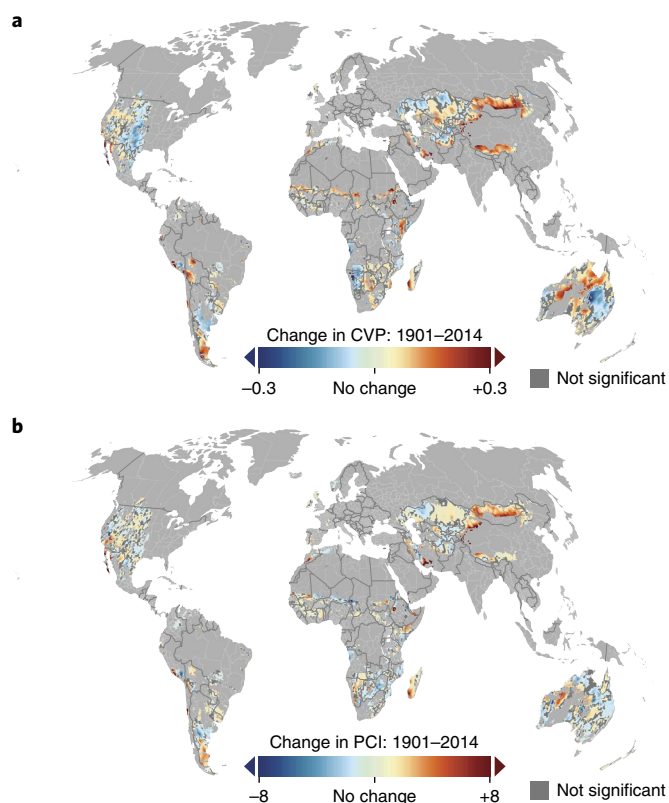


Fig. 2 | Overall, both within- and between-year precipitation variability has increased for global pasture areas. a, b. Here, we map changes in year-to-year precipitation variability as CVP (**a**) and changes in within-year precipitation distribution as the PCI (**b**) between 1901 and 2014. Plotted values reflect the slope of a linear regression fit to a sliding-window analysis in which values were calculated in sequential 25-year windows for the entire time period. Of the total land area considered pasture in this analysis, 20% did not experience significant changes in CVP (dark grey), 49% experienced significant increases in CVP (warm colours) and 31% experienced significant decreases in CVP (cool colours), $P < 0.05$. Of the total land area considered pasture in this analysis, 21% did not experience significant changes in PCI, whereas 45% experienced significant increases and 34% experienced significant decreases in PCI over the same time period.

grazing is less important (light red and light blue) have a lower CVP (0.20). Overall, CVP has increased over time in all areas ($P < 0.05$), although CVP trends appear to decrease in the more recent parts of the time series. The rates of CVP increase appear to be greatest in areas where livestock grazing may be important for local food access (Fig. 3, dark blue, +0.05).

Many of the regions in which moderate or high precipitation variability risks becoming even more variable are regions that support the planet's most vulnerable people. Over 90% of the planet's 1.3 billion poor people live in Asia and sub-Saharan Africa²³. Much of sub-Saharan Africa is arid or semi-arid, and precipitation variability in these areas is extremely high. Many of these areas (for example, the Sahel, Somalia, Kenya and so on) sit in the vulnerable range of precipitation variability. Although there is a patchwork of local precipitation trends within these areas, the general trend is increasing variability (Fig. 2), which may induce ecosystem transitions and pose a threat to the maintenance or expansion of livestock production.

Changes in precipitation variability can also lead to transitions in livestock production systems with unknown consequences for human and natural systems. Growing rain-fed crops in areas with increasing climate variability may be more risky

than raising livestock. Consequently, farmers and pastoralists in areas with increasing CVP may move from a mixed crop-livestock system to a rangeland only system, and, in times of drought, may require purchased feeds²⁴. These land-use changes can pose risks because they lead to changes in the composition of livestock diets and the ability of smallholders to keep herds alive when forage is scarce in the dry season. Challenges posed by precipitation variability have also contributed to a shift from communal to semicommercial land tenure systems in southern African rangelands²⁵, which may limit the possibility of livestock movement to take advantage of spatial heterogeneity to mitigate the effects of climate variability⁶.

Changes in precipitation variability are especially concerning in areas that may be near ecosystem thresholds. For example, many parts of Australia have seen CVP transitions to values above 0.33 during the past century. Here the variable climate results in frequent and intense droughts and wet periods, which are mainly attributed to El Niño and La Niña events, tropical cyclones and variations in coastal wind direction²⁶. Consequently, Australian graziers have found new ways to adapt to changing climate variability. Historically, livestock numbers were sustained during drought primarily by a reliance on supplemental feed, although this often led to economic losses and land degradation²⁷. More recently, many graziers have adopted more successful strategies, such as to maintain lower stocking rates that are adjusted to changes in feed availability at the first signs of drought, as well as delayed restocking after droughts to allow for pasture recovery²⁷. As precipitation variability continues to increase in other parts of the globe, we expect adaptive management techniques such as these to become more prevalent.

Although, in many parts of the world, livestock keepers may need to implement new strategies to deal with the declining ability of rangelands to support grazers, some systems may appear to show the potential to increase their capacity. A decrease in CVP trends should be interpreted with caution, as the ability to take advantage of the changing suitability of grazing lands may be practically limited, and the suitability for intensified natural grazing may need to be assessed locally within each region. Many natural grazing systems may already be at capacity or overgrazed. For example, although Namibia relies heavily on rain-fed natural vegetation and crop residues for grazing²⁸, CVP is large (>0.33). CVP trends show a decreasing variability in this area, but it is probably not decreasing enough to indicate that increased livestock densities might be supported. Some global grazing lands have a relatively low CVP paired with low cattle densities (light blue areas in Fig. 1a). Examples are found in parts of Kazakhstan, southern Australia and southern Argentina. However, an analysis of trends (Fig. 2) reveals a patchy mosaic of significant increases and decreases in precipitation variability within each of these areas. Additionally, the existence of low regional cattle densities and a favourably trending climate may not necessarily indicate areas where production could be sustainably increased. For example, many central Asian grasslands are still recovering from decades of overgrazing²⁹, and our analysis shows that this area exhibited significant declines in NDVI between 1982 and 2010 (Supplementary Fig. 12).

Both inter- and intra-annual precipitation variability are increasing on global pastures. Areas where grazing natural forage is important for food access and economies are especially affected. Visualizing spatially explicit patterns of CVP and PCI can help us identify areas that have undergone significant precipitation changes and learn from those areas that have managed to maintain production without degradation. Although the capacity for a landscape to support livestock depends on many factors in addition to climate, risk analysis using the metrics presented here can be used to target policy and management response to improve pasture resilience under a changing climate.

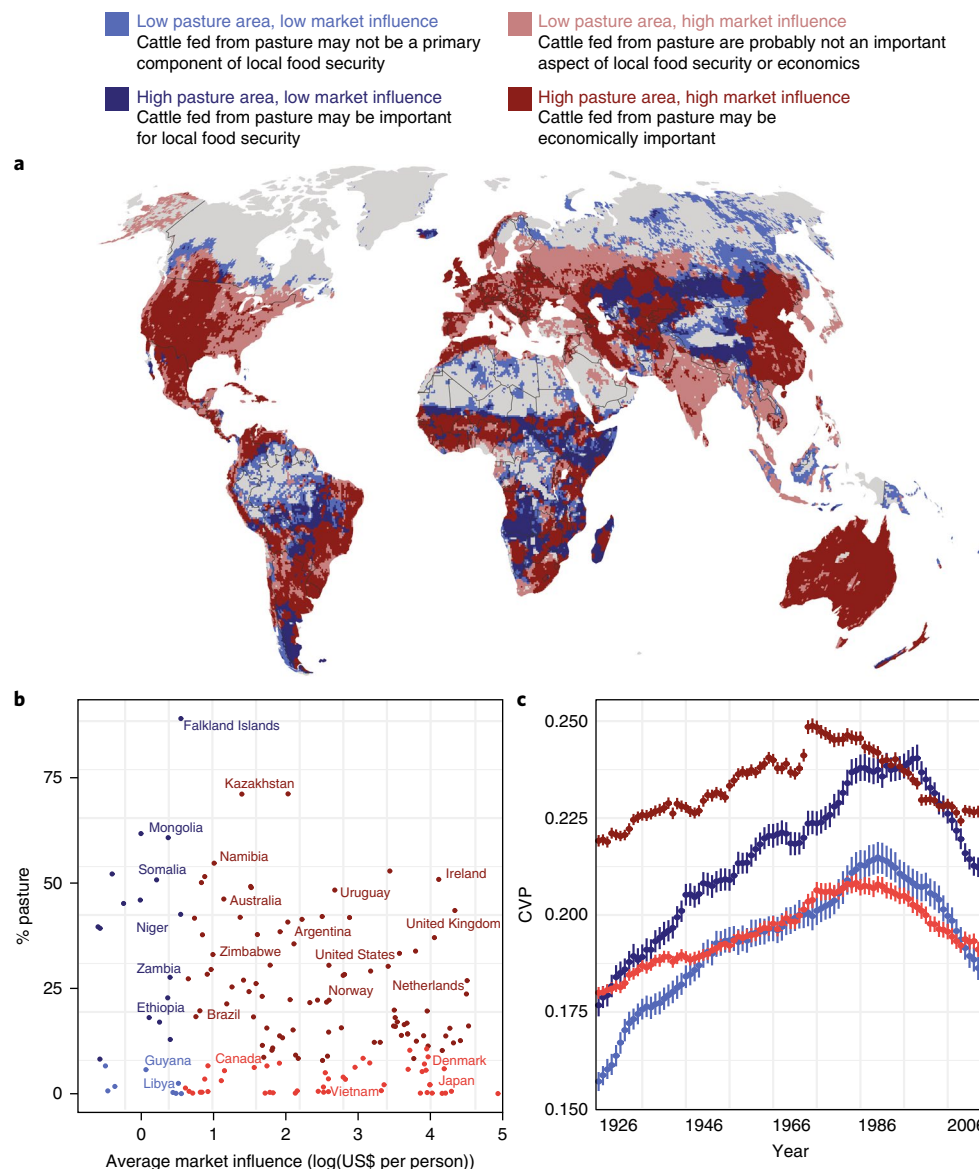


Fig. 3 | Where cattle fed from pasture are important, globally. a, b. Areas in which livestock grazing is important, economically or for food security, are mapped globally (**a**) and summarized by country (**b**). **c.** CVP trends between 1901 and 2014 are analysed for each region. The importance of livestock fed from pasture is defined by combining information on the amount of area devoted to pasture and the market influence (market access and personal purchasing power)²². CVP has increased significantly in all the regions (**c**, linear regression, $P < 0.05$); dark blue, +0.05; light blue, +0.04; dark red, +0.01; light red, +0.02. Overall CVP is highest in areas where livestock grazing is economically important (dark red, CVP = 0.238), but CVP has increased the most over the past century in areas where livestock grazing is suspected to be important for local food access (dark blue, +0.05).

Methods

Methods, including statements of data availability and any associated accession codes and references, are available at <https://doi.org/10.1038/s41558-018-0081-5>.

Received: 13 December 2016; Accepted: 16 January 2018;

Published online: 19 February 2018

References

- Galvin, K. A., Reid, R. S., Behnke, R. H. & Hobbs, N. T. *Fragmentation in Semi-Arid and Arid Landscapes: Consequences for Human and Natural Systems* (Springer: Amsterdam, 2018).
- O'Mara, F. P. The role of grasslands in food security and climate change. *Ann. Bot.* **110**, 1263–1270 (2012).
- Campbell, B. D. & Stafford Smith, D. M. A synthesis of recent global change research on pasture and rangeland production: Reduced uncertainties and their management implications. *Agric. Ecosyst. Environ.* **82**, 39–55 (2000).
- Herrero, M. et al. Biomass use, production, feed efficiencies, and greenhouse gas emissions from global livestock systems. *Proc. Natl Acad. Sci. USA* **110**, 20888–20893 (2013).
- Foley, J. A. et al. Solutions for a cultivated planet. *Nature* **478**, 337–342 (2011).
- Allred, B. W., Scasta, J. D., Hovick, T. J., Fuhlendorf, S. D. & Hamilton, R. G. Spatial heterogeneity stabilizes livestock productivity in a changing climate. *Agric. Ecosyst. Environ.* **193**, 37–41 (2014).
- Ellis, J. E. & Swift, D. M. Stability of African pastoral ecosystems: alternate paradigms and implications for development. *J. Range Manag.* **41**, 450–459 (1988).
- Briske, D. D., Fuhlendorf, S. D. & Smeins, F. E. Vegetation dynamics on rangelands: a critique of the current paradigms. *J. Appl. Ecol.* **40**, 601–614 (2003).
- Illius, A. W. & O'Connor, T. G. On the relevance of nonequilibrium concepts to arid and semiarid grazing systems. *Ecol. Appl.* **9**, 798–813 (1999).
- Asner, G. P., Elmore, A. J., Olander, L. P., Martin, R. E. & Harris, A. T. Grazing systems, ecosystem responses, and global change. *Annu. Rev. Environ. Resour.* **29**, 261–299 (2004).

11. IPCC *Climate Change 2014: Synthesis Report* (eds Core Writing Team, Pachauri, R. K. & Meyer L. A.) (IPCC, 2015).
12. Ellis, J. & Galvin, K. A. Climate patterns and land-use practices in the dry zones of Africa. *Bioscience* **44**, 340–349 (1994).
13. Wehrden, H. Von, Hanspach, J., Kaczensky, P., Fischer, J. & Wesche, K. Global assessment of the non-equilibrium concept in rangelands. *Ecol. Appl.* **22**, 393–399 (2012).
14. Le Houérou, H. N., Bingham, R. L. & Skerbek, W. Relationship between the variability of primary production and the variability of annual precipitation in world arid lands. *J. Arid Environ.* **15**, 1–18 (1988).
15. Knapp, A. K., Harper, C. W., Danner, B. T. & Lett, M. S. Rainfall variability, carbon cycling, and plant species diversity in a mesic grassland. *Science* **298**, 2202–2205 (2002).
16. Huxman, T. E. et al. Precipitation pulses and carbon fluxes in semiarid and arid ecosystems. *Oecologia* **141**, 254–268 (2004).
17. Oliver, J. E. Monthly precipitation distribution: a comparative index. *Prof. Geogr.* **32**, 300–309 (1980).
18. Sokol Jurkovic, R. & Zoran, P. Spatial variability of annual precipitation using globally gridded data sets from 1951 to 2000. *Int. J. Climatol.* **33**, 690–698 (2013).
19. Fatichi, S., Ivanov, V. Y. & Caporali, E. Investigating interannual variability of precipitation at the global scale: is there a connection with seasonality? *J. Clim.* **25**, 5512–5523 (2012).
20. Li, X., Jiang, F. & Wang, G. Spatial and temporal variability of precipitation concentration index, concentration degree and concentration period in Xinjiang, China. *Int. J. Climatol.* **31**, 1679–1693 (2011).
21. Marengo, J. A., Tomasella, J., Soares, W. R., Alves, L. M. & Nobre, C. A. Extreme climatic events in the Amazon basin. *Theor. Appl. Climatol.* **107**, 73–85 (2012).
22. Verburg, P. H., Ellis, E. C. & Letourneau, A. A global assessment of market accessibility and market influence for global environmental change studies. *Environ. Res. Lett.* **6**, 34019 (2011).
23. Thornton, P. et al. Vulnerability, climate change and livestock—research opportunities and challenges for poverty alleviation. *SAT eJournal* **4**, 1–23 (2007).
24. Jones, P. G. & Thornton, P. K. Croppers to livestock keepers: livelihood transitions to 2050 in Africa due to climate change. *Environ. Sci. Policy* **12**, 427–437 (2009).
25. Dube, O. P. & Pickup, G. Effects of rainfall variability and communal and semi-commercial grazing on land cover in southern African rangelands. *Clim. Res.* **17**, 195–208 (2001).
26. Cleverly, J. et al. The importance of interacting climate modes on Australia's contribution to global carbon cycle extremes. *Sci. Rep.* **6**, 23113 (2016).
27. Landsberg, R. G., Ash, A. J., Shepherd, R. K. & McKeon, G. M. Learning from history to survive in the future: management evolution on Trafalgar Station, north-east Queensland. *Rangel. J.* **20**, 104–118 (1998).
28. Newsham, A. J. & Thomas, D. S. G. Knowing, farming and climate change adaptation in North-Central Namibia. *Glob. Environ. Chang.* **21**, 761–770 (2011).
29. Mirzabaev, A., Ahmed, M., Werner, J., Pender, J. & Louhaichi, M. Rangelands of Central Asia: challenges and opportunities. *J. Arid Land* **8**, 93–108 (2016).

Acknowledgements

L.L.S., L.H.S., J.S.G., P.C.W. and L.G.F. acknowledge the support from the Gordon and Betty Moore Foundation. M.H. and C.G. acknowledge support from the CSIRO Science Leaders Programme. J.S.G., P.C.W. and M.H. were supported by the Belmont Forum/FACCE-JPI funded DEVIL project (Delivering Food Security from Limited Land) (NE/M021327/1) via NSF award no. 1540195. L.L.S. thanks the Early Career Cross-Disciplinary Writing Group.

Author contributions

L.L.S., L.H.S., J.S.G. and P.C.W. conceived the idea of the study; W.K.S. and L.G.F. contributed to the remote sensing analysis; J.S.G. helped with coding and analysis; M.H. contributed with livestock density data and grazing concepts; C.G. and L.H.S. helped with the literature review; L.L.S. analysed the data and wrote the manuscript. All the authors contributed to the discussions and writing or revision of the manuscript.

Additional information

Supplementary information is available for this paper at <https://doi.org/10.1038/s41558-018-0081-5>.

Reprints and permissions information is available at www.nature.com/reprints.

Correspondence and requests for materials should be addressed to L.L.S.

Publisher's note: Springer Nature remains neutral with regard to jurisdictional claims in published maps and institutional affiliations.

Methods

Data. *Climate data.* Monthly average precipitation and temperature data at 30-minute (0.5°) resolution were obtained from the Climatic Research Unit (CRU TS v. 3.23)³⁰. We chose to present results from the CRU precipitation data set because it is one of the most widely used interpolated data sets and possibly the best-available precipitation data set for larger scales³¹. The data span 1901 to 2014. Precipitation data come from over 4,000 meteorological stations and are interpolated based on spatial autocorrelation functions but are not forced with climate models. Monthly average shortwave downward radiation data were obtained from the CRU-NCEP v. 6 data set, at the same spatial resolution as the CRU climate data. CRU and CRU-NCEP data are freely available online. Any locations for which precipitation is filled by static annual averages at any point in the time series were removed from analysis.

There is some uncertainty in the determination of CVP due to the choice of precipitation product and inhomogeneity due to the variability in the number of stations and data quality over time. In an effort to address this, we mapped the agreement between the CRU data set used in this analysis and two other global, interpolated precipitation data sets: Global Precipitation and Climatology Center³² and University of Delaware Precipitation³³ (Supplementary Figs. 3 and 4). These additional data sets were chosen because they are (1) based on station data and (2) cover the same time series as the CRU data.

Pasture area. We used a global map of per cent pasture for the year 2010 (D. Plouffe & N. Ramankutty, personal communication). This new data set was developed using an approach similar to that of Ramankutty et al.³⁴, but using an updated methodology, and by calibrating land cover from Boston University based on the moderate-resolution imaging spectroradiometer (MODIS) satellite against a global compilation of agricultural census statistics. Although Ramankutty et al.³⁴ used the final classified MODIS land-cover data set, this data set uses the posterior land-cover probabilities that are calculated in the process of making the MODIS land-cover product, which results in a greater accuracy in the spatial patterns of the final pasture maps.

We used a combination of the per cent pasture map and the global livestock production systems (GLPS) map for the year 2011³⁵ to define a binary pasture mask. A 0.5° grid cell was generally considered pasture if it fell into a livestock category on the GLPS map and also contained at least 30% pasture by area.

Bovine density. Global maps of bovine density for the year 2006 were obtained from published data⁴. Animal numbers come from the Food and Agriculture Organization (FAO). Data were provided at a 5-minute resolution and aggregated to a 30-minute (0.5°) resolution.

Vegetation productivity. Global NDVI data were obtained from the Advanced Very High-Resolution Radiometer Global Inventory Modeling and Mapping Studies (GIMMS) data set³⁶. The data set provides monthly NDVI from 1982 to 2010 at a 5-minute resolution and data (average annual values) were aggregated to a 30-minute (0.5°) resolution. Many studies have found that NDVI is highly correlated with above-ground plant productivity^{37–42}. Therefore, NDVI is generally accepted as a basis to assess trends in vegetation productivity. The GIMMS NDVI data set is freely available online.

Analyses. Analyses were completed in Matlab 2015b and 'R' v. 3.2.3.

Sliding-window analysis. CVP was calculated as the standard deviation divided by the mean of annual precipitation for the full time series. The change in CVP over time was calculated using a sliding-window analysis. This technique was chosen to reduce the influence of outliers and highlight longer-term trends. CVP was calculated in 25-year windows sliding by one time step after each calculation and ending after the last complete 25-year window. Consequently, a time series of CVP using precipitation data from 1901 to 2014 starts in 1926 and the CVP value for 1926 reflects interannual precipitation variability over the previous 25 years. MAP data were centred (value minus mean) before analysis. A simple linear regression was calculated for each grid cell on sliding-window CVP values over all time steps. The change in CVP is represented by model slopes. The change in CVP was reported as the slope of the linear regression multiplied by the length of x ($x=89$ because there are 114 years and 25-year windows). Significant models were determined by model P values <0.05 .

To quantify the uncertainty of CVP estimates, and the relationship of that uncertainty to window size, we tested our ability to recover trends correctly by analysing synthetic precipitation data sets whose statistical properties are specified. We used Fourier analysis to construct 10,000 realizations of 114-year annual precipitation data sets with known changes in CVP. We first calculated a global average precipitation spectrum from the CRU annual precipitation data on points with good data quality for at least 110 years. This calculation was carried out at each pixel using a discrete Fourier transform (DFT) in Matlab after zero padding⁴³ to 256 years. The absolute values of the resulting transforms were averaged to produce a single annual precipitation spectrum that contains a realistic representation of the temporal structure of the interannual correlation in precipitation patterns. Using an inverse

DFT, the non-zero-frequency spectral components were reassembled with random uncorrelated Hermitian phases to construct a zero-mean realization of annual precipitation. Each of 10,000 realizations was multiplied by linear ramps (with increases and decreases of 20%, 30%, 40%, 50%, 60% and 70%) and increased by a constant, which results in a precipitation series with the desired properties (namely, a constant mean, linearly varying coefficient of variation). Under this scenario, with a 25-year window size, a 20% change in CVP can be detected with an ~8% chance of false positives, and a 70% change in CVP can be detected with a ~2.3% chance of false positives (Supplementary Fig. 8).

PCI was calculated using this equation¹⁷ in which p (mm) is the total monthly precipitation:

$$PCI_{\text{annual}} = \frac{\sum_{i=1}^{12} p_i^2}{\left(\sum_{i=1}^{12} p_i\right)^2} \times 100$$

Changes in PCI were calculated using the same sliding-window approach as described above. The benefit of this index includes the fact that the index is bounded, which allows for a direct comparison between locations, irrespective of the total precipitation. The PCI does not, however, identify temporal aspects of seasonal rainfall. Although potentially important, an analysis of these changes falls outside the scope of this article, but would make a valuable contribution to future climate risk work.

Climate model selection. AIC model competition was used to find the model that best explains changes in NDVI between 1982 and 2011 for each 0.5° grid cell using four explanatory variables: MAT, MAP, mean annual downward solar radiation and CVP. All possible combinations of explanatory variables (without interaction terms) were computed and the model with the lowest AIC score was retained, using the MuMin package in 'R'⁴⁴. Supplementary Information contains a categorical map of where each model type is found globally (Supplementary Fig. 6) as well as the corresponding map of model R^2 values (Supplementary Fig. 7). A summary of the frequency of variable retention is presented in Supplementary Table 1.

Data availability. The temperature and precipitation data used in this study are available from <https://crudata.uea.ac.uk/cru/data/hrg/>. The monthly average shortwave downward radiation data were obtained from the CRU-NCEP v. 6 data set available at https://crudata.uea.ac.uk/cru/data/ncep/#dataset_access. The precipitation data sets used for comparison are available at www.esrl.noaa.gov/psd/data/gridded/data.gpcp.html and www.esrl.noaa.gov/psd/data/gridded/data.UDEL_AirT_Precip.html. The NDVI data used in this study are available from <https://ecocast.arc.nasa.gov/data/pub/gimms/3g.v0/>, and the bovine density data⁴ are available from the corresponding authors on reasonable request. The 'market influence' data used in this study are available at www.ivm.vu.nl/marketinfluence. The percent pasture map for the year 2010 is available on reasonable request to the corresponding author. The Food and Agriculture Organization GLPS map is available at www.fao.org/geonetwork.

References

- Harris, I., Jones, P. D., Osborn, T. J. & Lister, D. H. Updated high-resolution grids of monthly climatic observations—the CRU TS3.10 Dataset. *Int. J. Climatol.* **34**, 623–642 (2014).
- Koutsouris, A. J., Chen, D. & Lyon, S. W. Comparing global precipitation data sets in eastern Africa: a case study of Kilombero Valley, Tanzania. *Int. J. Energy* **36**, 2000–2014 (2016).
- Becker, A. et al. A description of the global land-surface precipitation data products of the Global Precipitation Climatology Centre with sample applications including centennial (trend) analysis from 1901–present. *Earth Syst. Sci. Data* **5**, 71–99 (2013).
- Legates, D. R. & Willmott, C. J. Mean seasonal and spatial variability in gauge-corrected, global precipitation. *Int. J. Climatol.* **10**, 111–127 (1990).
- Ramankutty, N., Evan, A. T., Monfreda, C. & Foley, J. A. Farming the planet: 1. Geographic distribution of global agricultural lands in the year 2000. *Global Biogeochem. Cycles* **22**, 1003 (2008).
- Robinson, T. P. et al. *Global Livestock Production Systems* (Food and Agriculture Organization of the United Nations FAO, Rome, 2011).
- Zeng, F. W., James Collatz, G., Pinzon, J. E. & Ivanoff, A. Evaluating and quantifying the climate-driven interannual variability in global inventory modeling and mapping studies (GIMMS) normalized difference vegetation index (NDVI3g) at global scales. *Remote Sens.* **5**, 3918–3950 (2013).
- Fensholt, R., Nielsen, T. T. & Stisen, S. Evaluation of AVHRR PAL and GIMMS 10-day composite NDVI time series products using SPOT-4 vegetation data for the African continent. *Int. J. Remote Sens.* **27**, 2719–2733 (2006).

- 38 Fensholt, R. & Rasmussen, K. Analysis of trends in the Sahelian 'rain-use efficiency' using GIMMS NDVI, RFE and GPCP rainfall data. *Remote Sens. Environ.* **115**, 438–451 (2011).
- 39 Fensholt, R., Rasmussen, K., Nielsen, T. T. & Mbow, C. Evaluation of earth observation based long term vegetation trends—intercomparing NDVI time series trend analysis consistency of Sahel from AVHRR GIMMS, Terra MODIS and SPOT VGT data. *Remote Sens. Environ.* **113**, 1886–1898 (2009).
- 40 Prince, S. D. Satellite remote sensing of primary production: comparison of results for Sahelian grasslands 1981–1988. *Int. J. Remote Sens.* **12**, 1301–1311 (1991).
- 41 Groten, S. M. E. NDVI—crop monitoring and early yield assessment of Burkina Faso. *Int. J. Remote Sens.* **14**, 1495–1515 (1993).
- 42 Box, E. O., Holben, B. N. & Kalb, V. Accuracy of the AVHRR vegetation index as a predictor of biomass, primary productivity and net CO₂ flux. *Vegetatio* **80**, 71–89 (1989).
- 43 Press, W. H., Teukolsky, S. A., Vetterling, W. T. & Flannery, B. P. *Numerical Recipes: The Art of Scientific Computing* 3rd edn (Cambridge University Press, Cambridge, 2007).
- 44 Barton, K. Package 'MuMIn' v.1.40.0 (2015).